

Simulation and analysis of co-phasing errors of the segmented primary mirror tiled by hexagonal segments in LOT

Shi-Dong Shen^{1,2,3}, Xiang-Qun Cui^{1,2} and Yong Zhang^{1,2}

¹ National Astronomical Observatories/Nanjing Institute of Astronomical Optics & Technology, Chinese Academy of Sciences, Nanjing 210042, China; xcui@niaot.ac.cn

² CAS Key Laboratory of Astronomical Optics & Technology, Nanjing Institute of Astronomical Optics & Technology, Nanjing 210042, China

³ University of the Chinese Academy of Sciences, Beijing 100049, China

Received 2020 December 1; accepted 2021 June 3

Abstract In this paper, co-phasing errors of a segmented primary mirror tiled by hexagonal segments are successfully calculated for the 12-meter Large aperture Optical/infrared Telescope (LOT). Co-phasing errors including out-of-plane errors are simulated separately and comprehensively based on several software simulation platforms. PAOLA simulation results show that the Strehl Ratio (SR) of LOT is larger than 0.8 when the RMS value of tip-tilt obeying a normal distribution is less than 0.018 arcsec, and the SR of LOT is larger than 0.8 when the RMS value of piston obeying a normal distribution is less than 40 nm. Besides, simulation results of Zemax show that the SR of LOT is larger than 0.8 when the RMS value of tip-tilt obeying a normal distribution is less than 0.02 arcsec, and the SR of LOT is larger than 0.8 when the RMS value of piston obeying a normal distribution is less than 40 nm. These simulation results successfully lay a solid foundation for LOT (especially the segmented primary mirror with active optics).

Key words: methods: analytical — techniques: miscellaneous — telescopes

1 INTRODUCTION

With the rapid development of astronomical science and the urgent need for large aperture telescopes with higher light collecting capacity and resolution, many large/extremely large aperture optical-infrared telescopes have been built or are under construction around the world. In order to build a larger aperture telescope, segmented mirror active optics in which a large number of segments are used to assemble a whole large aperture mirror has become the first choice considering the influence of all factors such as technical difficulty, cost and fabrication cycle (Su & Cui 2004).

A group of international 8–10 meter aperture optical telescopes has been built from the 1990s, which mainly include: Subaru, VLT, LBT, Gemini, Keck, HET, GTC and SALT. Countries have begun to develop 30-meter telescopes, such as GMT, TMT and ELT in the past decade. This ushers ground-based large aperture optical-infrared telescopes into a new era.

The primary mirror of the Keck telescope consists of 36 hexagonal segments with side length of 900 mm.

There is an average gap of 3 mm between adjacent segments which have thickness of 75 mm. Keck reaches co-focus in visible waveband at present, and co-phase can be achieved at 1.1–2.3 μm with the help of adaptive optics (AO). The root mean square (RMS) value of tip-tilt is less than 0.018 arcsec, and the RMS value of piston is less than 30 nm (Nelson & Gillingham 1994; Su & Cui 1999; Chanan et al. 2000, 1998; Troy et al. 1998; Gleckler & Wizinowich 1995).

TMT, designed for a waveband of 300 nm–30 μm , is the leader in the next generation of extremely large aperture optical-infrared telescopes. The resolution of TMT in the waveband of 300–1000 nm is limited by atmospheric seeing, and TMT can achieve diffraction limited imaging at 1000 nm with the planned AO system. The primary mirror of TMT has a diameter of 30 m, which consists of 492 hexagonal segments with diagonal length of 1440 mm, thickness of 45 mm and gap of 2.5 mm. The co-phasing process of TMT is divided into two steps including the coarse co-phasing process and fine co-phasing process. Low order aberrations are corrected in the coarse co-phasing process, making the

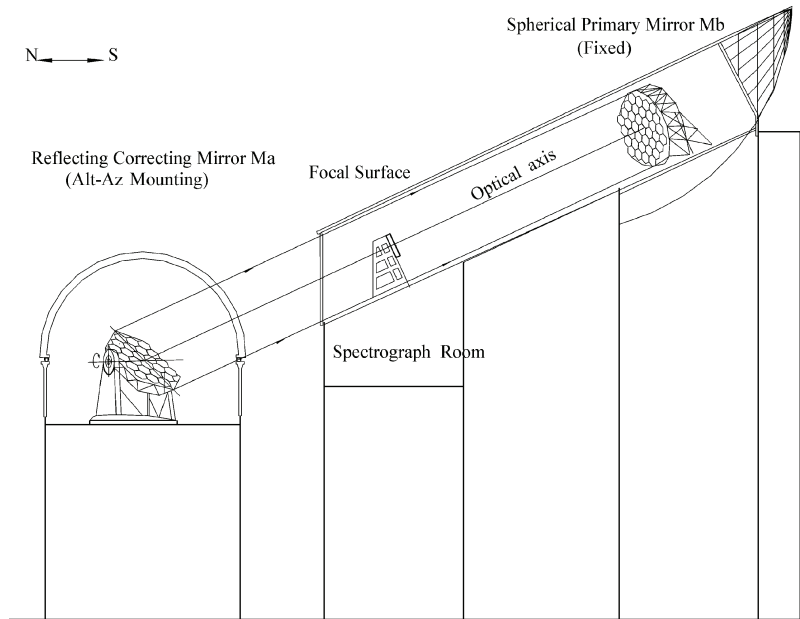


Fig. 1 3D structure map of LAMOST (Su & Cui 2004).

RMS value of the wavefront of TMT decrease from $40\ \mu\text{m}$ to $400\ \text{nm}$. The RMS value of piston is about $30\ \text{nm}$ after the fine co-phasing process (Nelson 2000; Ellerbroek et al. 2005; Baffes et al. 2008; Sanders 2013; Piatrou & Chanan 2011). Mitchell Troy and Gray Chanan from USA analyzed the influence of gaps, secondary mirror obstruction and reflectivity of mirrors on the performance of TMT (Troy & Chanan 2003).

The first six hexagonal segments of the primary mirror in ELT have been successfully cast by the SCHOTT company in 2018, and ELT will see first light in 2024. The primary mirror diameter of ELT is $39\ \text{m}$, which is tiled by 798 segments, each with diagonal length of $1450\ \text{mm}$, central thickness of $50\ \text{mm}$ and gap of $4\ \text{mm}$. ELT will achieve co-phase in the near-infrared waveband with the help of AO (McPherson et al. 2012). N. Yaitskova from European Southern Observatory derived the analytical expression for formulas describing highly segmented telescopes, and established an optical calculation model of point spread function (PSF) based on fast Fourier transform, and simulated the influence of piston error and tip-tilt error on the Strehl Ratio (SR) of the telescope, providing data support for the active control of ELT (Yaitskova & Dohlen 2000).

LAMOST that is displayed in Figure 1 is the largest segmented mirror telescope in China and the largest wide field segmented mirror telescope in the world at present. LAMOST is mainly composed of a Schmidt correction mirror Ma with real-time deformable segments and spherical primary mirror Mb. In addition, LAMOST

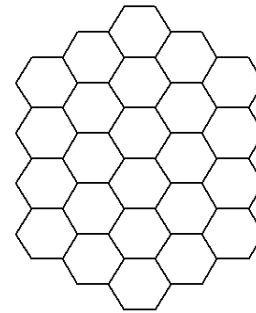


Fig. 2 Ma mirror of LAMOST.

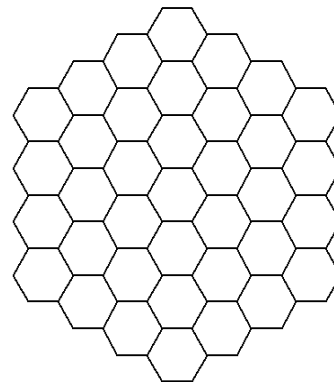


Fig. 3 Mb mirror of LAMOST.

is the only telescope with two segmented mirrors in the world.

The size of Ma displayed in Figure 2 is $5720\ \text{mm} \times 4400\ \text{mm}$, in which 24 segments are composed of

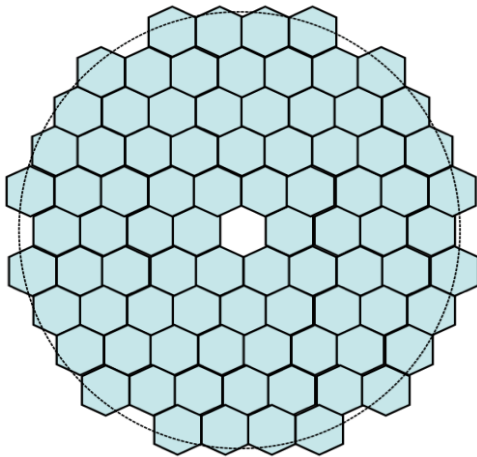


Fig. 4 Diagram of LOT primary mirror.

regular hexagonal flat mirrors with diagonal length 1100 mm and thickness 25 mm. Ma adopts thin mirror active optics and segmented mirror active optics. There are three displacement actuators and 34 force actuators behind a segment. Displacement actuators change the tilt of segments. Force actuators correct the gravity deformation and thermal deformation of segments, and produce real-time surface shape variation needed for the correction of spherical aberration from Mb.

The size of Mb displayed in Figure 3 is 6670 mm × 6050 mm, and there are 37 hexagonal spherical segments. The radius of curvature of a segment is 40 m, the diagonal length is 1100 mm and the thickness is 75 mm. Active optics technology is adopted, and the co-focus of Mb is realized by a Shack-Hartmann (SH) wavefront sensor at the spherical center of Mb and displacement actuators behind Mb (Su & Wang 1997; Zhang et al. 2014a; Wang et al. 1996).

The active optics team of Nanjing Institute of Astronomical Optics and Technology led by Su Ding-Qiang conducted an experiment with a system of segmented mirror active optics, in which the diffraction limit was reached at 650 nm (Su et al. 2000b). Zhang Yong tested co-phase active optics with three segments from Mb in the near-infrared waveband since 2009. The diffraction limit was reached at 1550 nm and SR was 0.806 when the RMS value of piston was 20 nm and the RMS value of tip-tilt was 0.03 arcsec (Zhang et al. 2014b). This achievement has made an important breakthrough in the core technology of active optics in China and promotes the construction of Chinese large optical-infrared telescopes and the development of related key technologies.

Su Ding-Qiang, Wang Ya-Nan and Cui Xiang-Qun proposed the Chinese Future Giant Telescope (CFGT), which includes a Nasmyth system, Coudé system and wide field system. The Nasmyth system is a Ritchey-Chrétien

(R-C) system, the focal ratio of which is 18 and field of view is 8 arcmin. Diameter of the primary mirror is 30 m, and focal ratio is 1.2. The hyperboloidal primary mirror has 17 rings and 1020 segments (Cui et al. 2003; Li et al. 2004). The co-phasing requirement is to meet diffraction limit at 2.1 μm . The requirement for the RMS value of tip-tilt is 0.03 arcsec and the RMS value of piston is 50 nm (Wang 2015).

In addition, Yunnan Observatories proposed the Chinese Giant Solar Telescope (CGST), the 8-meter primary mirror of which is tiled by fan-shaped segments. It is hoped that co-phase of the primary mirror is realized in the near-infrared waveband, such as 1 μm , and even in the visible waveband, such as 500 nm (Liu et al. 2019).

Chinese large general optical telescopes mainly include the National Astronomical Observatories 2.16-meter telescope and the Yunnan Astronomical Observatories 2.4-meter telescope. China has been studying the conceptual design and key technologies of a 30-meter extremely large telescope since the beginning of the 21st century (Su et al. 2000a, 2004). At present, China is in urgent need for large aperture universal optical telescopes to improve the capacity of astronomical observation in the optical-infrared waveband, so the LOT has been proposed which is of great significance to Chinese astronomy (Su et al. 2016). The 12-meter primary mirror of LOT will also adopt segmented mirror active optics to realize co-phase in both visible and near-infrared wavebands. The correction for the segmented primary mirror includes tip-tilt correction and piston correction of segments. The successful experience of active optics in Keck will be followed by LOT. An SH wavefront sensor will be employed to detect tip-tilt and piston errors of segments in LOT based on image stabilization with AO.

At present, basic principles and methods of co-phasing error analysis are as follows: theoretical expression of PSF of a telescope can be obtained from the perspective of physical optics, and the relationship between co-phasing errors and SR is deduced, and values of co-phasing errors are given. Point diagram, SR and modulation transfer function (MTF) of a telescope can be obtained to characterize image quality of the telescope based on the ray tracing simulation of geometric optics.

Error analysis and simulation are the prerequisites and necessary conditions for error allocation during the feasibility evaluation for any large aperture segmented telescope. This study is of great significance for the construction of LOT, which is major national scientific and technological infrastructure. Near-infrared co-phasing wavelength of LOT is chosen as 1 μm in this paper, and the simulation analysis is carried out for the co-phasing error in LOT.

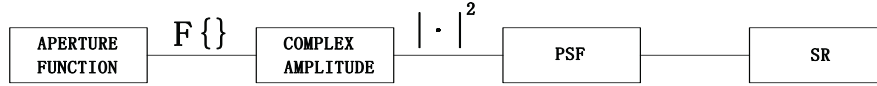


Fig. 5 Relation between aperture function and SR.

2 ANALYSIS OF CO-PHASING ERRORS

Hexagonal segments are widely incorporated in large aperture segmented mirror telescopes. The current segmentation program of LOT is that the primary mirror is divided into 84 hexagonal segments with side length 720 mm in order to ensure light gathering ability of the 12-meter primary mirror and take advantage of manufacturing experience and facilities which have been mastered by Nanjing Institute of Astronomical Optics & Technology in manufacturing segments of the primary mirror of TMT (Su et al. 2017). The specific schematic diagram is displayed in Figure 4.

Co-phasing errors in segmented mirrors are mainly divided into segmentation errors and manufacturing errors. Segmentation errors mainly include piston and tip-tilt (three) out-plane errors and decenter x , decenter y and clocking (three) in-plane errors. Manufacturing errors include conformity to the radius of curvature of segments, surface misfigure error in the manufacturing process and turned down edges of segments (Ming et al. 2009; Wan et al. 2007). Calculation and simulation of various errors will be of great importance in the development of LOT before the design and installation of segmented mirrors.

The in-plane degrees of freedom are often subject to the passive constraint of the supporting structure of segments, so that there is no need for in-plane errors after installation of segments. The other three out-of-plane degrees of freedom are corrected by active optics (Mast & Nelson 1982). The influence of the three out-of-plane degrees of freedom will be mainly analyzed in this paper.

PSF is the most effective image quality evaluation index in the field of astronomical optics, but the most commonly used quantitative index is SR. SR greater than 0.8 or RMS value of wavefront of LOT less than 0.075λ will be used as the evaluation standard for the co-phase status of the primary mirror in theoretical calculation and simulation analysis in this paper (Lightsey & Chrisp 2003).

The theoretical flow chart from co-phasing errors to SR is depicted in Figure 5, and the final SR is obtained after Fourier transform and related calculation by adding some co-phasing errors to the aperture function.

First of all, the influence of tip-tilt of segments is analyzed. Tip-tilt will only change PSF of a segment

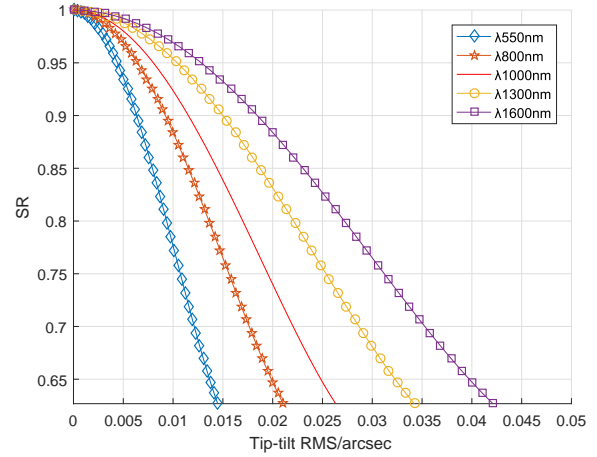


Fig. 6 Relation between SR and the RMS value of tip-tilt at different wavelengths.

but not change the grid factor function of the segmented primary mirror as a segment rotates around the center of itself. Assuming that β represents tilt angle, and tip error is normally distributed and tilt error is normally distributed, and these quantities are independent of each other, and RMS_β (in radian units, rad) indicates the RMS value of tip-tilt in LOT, we can obtain (Yaitskova & Dohlen 2002)

$$SR = 1 - 3.412 \times 10^{13} \text{RMS}_\beta^2 + 6.881 \times 10^{26} \text{RMS}_\beta^4. \quad (1)$$

Relation between SR and the RMS value of tip-tilt at different wavelengths is drawn in Figure 6. According to the calculation results, the SR is larger than 0.8 when the RMS value of tip-tilt is less than 0.017 arcsec when the co-phasing wavelength of LOT is $1 \mu\text{m}$.

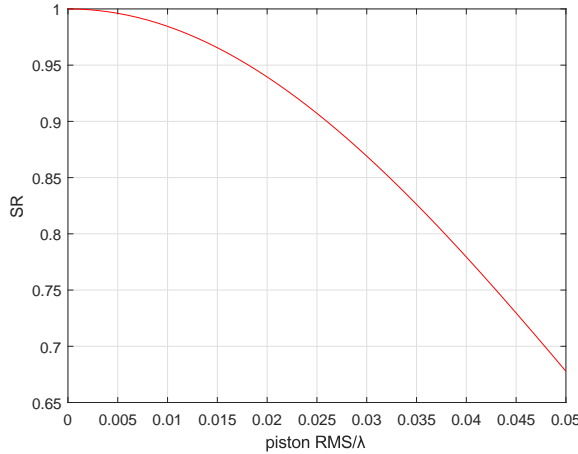
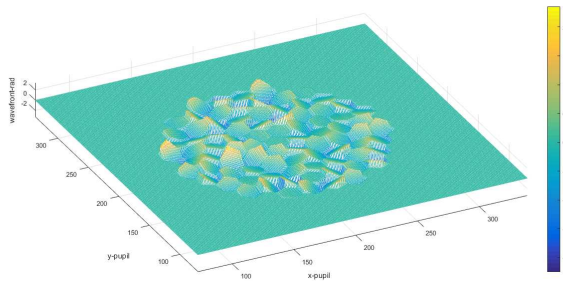
Piston is the translation error along the normal direction of a segment center. Piston does not change the PSF of a segment but changes the periodic structure of the grid factor function of the primary mirror in LOT. Assuming that the pistons of segments are independent of each other and follow a normal distribution, and RMS_{pe} (in wavelength units, λ) indicates the RMS value of piston, we can obtain (Yaitskova & Dohlen 2000)

$$SR = 0.012 + 0.988 \exp \left[- \left(\frac{4\pi}{\lambda} \text{RMS}_{pe} \right)^2 \right]. \quad (2)$$

Relationship between SR and the RMS value of piston is drawn in Figure 7. SR would be larger than 0.8 when the RMS value of piston is less than 37.8 nm based on the calculation results when the co-phasing wavelength of LOT is $1 \mu\text{m}$.

Table 1 Influence of Tip-tilt on the SR of the Primary Mirror

| Theoretical SR of the primary mirror | Theoretical RMS value of tip-tilt (arcsec) | RMS value of tip-tilt in simulation (arcsec) | SR in simulation |
|--------------------------------------|--|--|------------------|
| 0.95 | 0.008 | 0.01 | 0.93 |
| 0.9 | 0.012 | 0.015 | 0.842 |
| 0.85 | 0.015 | 0.017 | 0.81 |
| 0.81 | 0.017 | 0.018 | 0.8 |
| 0.8 | 0.017 | 0.02 | 0.77 |
| 0.7 | 0.022 | 0.025 | 0.64 |

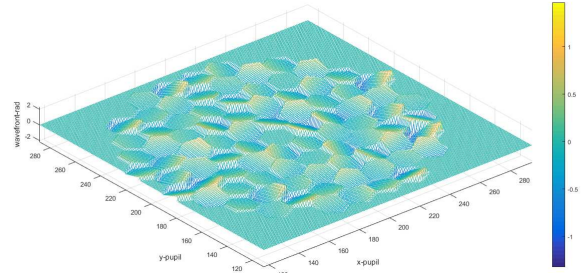
**Fig. 7** Relationship between SR and the RMS value of piston.**Fig. 8** Three-dimensional (3D) phase diagram of segments in the primary mirror (SR is 0.8 when the RMS value of tip-tilt is 0.018 arcsec).

3 SIMULATION RESULTS OF CO-PHASING ERRORS IN LOT

3.1 Simulation of Co-phasing Errors Separately

The real co-phasing errors should be simulated as final reference and comparative verification of theoretical calculation in the development of LOT. The PAOLA program (Jolissaint 2010) firstly simulates tip-tilt, and results are displayed in Table 1.

According to the actual simulation results by the PAOLA program, the SR of the primary mirror is larger than 0.8 when the RMS value of tip-tilt is less than 0.018

**Fig. 9** 3D phase diagram of segments in the primary mirror (SR is 0.93 when the RMS value of tip-tilt is 0.01 arcsec).

arcsec. The simulation result about the RMS value of tip-tilt is slightly larger than the theoretical RMS value and close to the angular resolution of 0.021 arcsec for the 12-meter primary mirror when the co-phasing wavelength is 1 μm . The phase of each segment is depicted in Figure 8 when the RMS value of tip-tilt is 0.018 arcsec, and the phase of each segment is shown in Figure 9 when the RMS value of tip-tilt is 0.01 arcsec.

Monte Carlo analysis is a numerical calculation method guided by probability and statistics theory. Numerical characteristics of the model are calculated by a statistical method by generating random numbers conforming to a certain probability distribution. This approach has been widely applied in the field of numerical calculation. Tolerance analysis in Zemax is realized through Monte Carlo analysis. The probability distribution model and operation time and other parameters for tolerance analysis need to be set up in the tolerance analysis setting page in Zemax. Probability and statistical distribution can be selected as normal distribution, uniform distribution and so on. The distribution range is generally selected as 4 times the standard deviation if the tolerance operands obey a normal distribution (Geary 2002).

Tip-tilt of 84 hexagonal segments is applied to the same normal distribution in local coordinate system for segments in Zemax software as seen in Figure 10, and the width is 2σ (σ is the standard deviation and the RMS value of the tilt angle). The two ends of the width are equal to the maximum and minimum values of the tolerance operands. The RMS value of wavefront less than 0.075λ is the error evaluation criterion. The result is that the RMS value of the

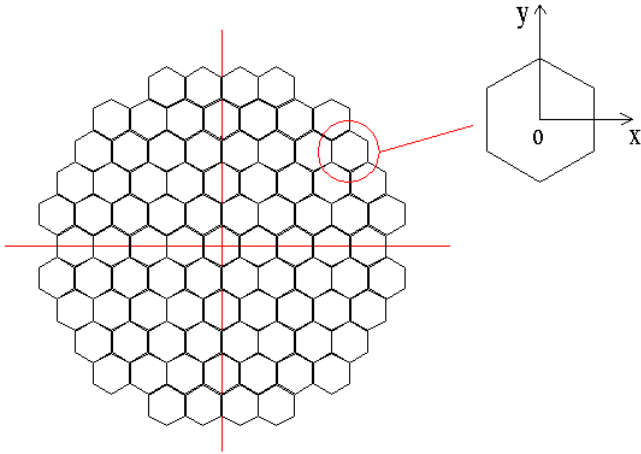


Fig. 10 Local coordinate system for segments in Zemax software.

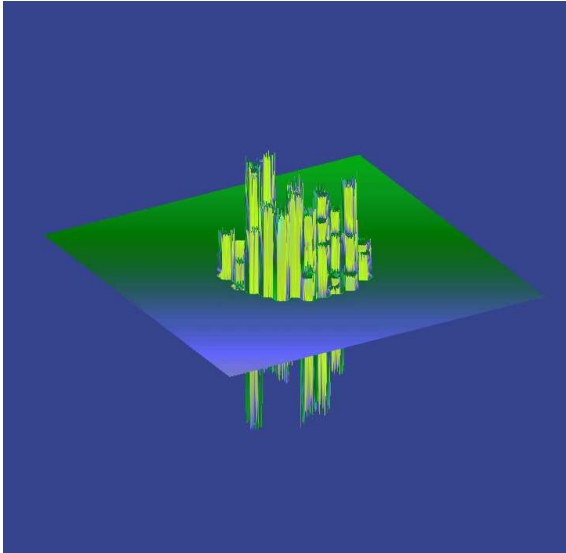


Fig. 11 3D phase diagram of the primary mirror (SR is 0.8 when the RMS value of piston is 40 nm).

wavefront during 90% of stochastic simulation processes is less than 0.073λ (λ is $1 \mu\text{m}$) when the RMS value of tip-tilt is 0.02 arcsec, which obeys a normal distribution.

Secondly, the simulation of piston is performed and the simulation results based on PAOLA are displayed in Table 2.

SR of the primary mirror is 0.806 when the RMS value of piston is 40 nm according to the simulation results, and the wavefront of the primary mirror is shown in Figure 11 at the same time. The wavefront of the primary mirror is displayed in Figure 12 when the RMS value of the piston is 20 nm.

Pistons for 84 hexagonal segments are applied to the same normal distribution in Zemax software, and the width is 2σ (σ is the standard deviation and the RMS value

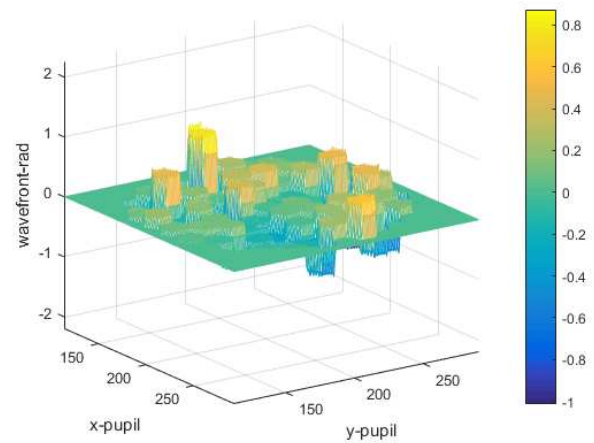


Fig. 12 3D phase diagram of the primary mirror (SR is 0.93 when the RMS value of piston is 20 nm).

of piston). The two ends of the width are equal to the maximum and minimum values of the tolerance operands. RMS value of the wavefront less than 0.075λ is the error evaluation criterion. The results affirm that the RMS value of wavefront of LOT is less than 0.075λ (λ is $1 \mu\text{m}$) in 90% of the random simulation processes when the RMS value of a normally distributed piston error is 40 nm.

3.2 Simulation of Co-phasing Errors

The factors of tip-tilt and piston exist, so in the actual situation a comprehensive co-phasing error simulation of the primary mirror would be needed. Comprehensive simulation analysis based on PAOLA is shown in Table 3. The PAOLA simulation is under the condition that the RMS value of tip-tilt, 0.012 arcsec, and the RMS value of piston, 26.6 nm, exist at the same time. The phase diagram of the wavefront of the primary mirror is displayed in Figure 13. The phase diagram of the wavefront of the primary mirror is depicted in Figure 14 when the RMS value of tip-tilt is 0.014 arcsec and the RMS value of piston is 32.3 nm.

It can be seen that the comprehensive simulation results based on the PAOLA program are basically close to the theoretical derivation. The RMS value of tip-tilt should be less than 0.012 arcsec and the RMS value of piston is required to be less than 26.6 nm under the influence of equal weighting factor from Table 3.

The simulation result is that the RMS value of tip-tilt needs to be less than 0.015 arcsec when the RMS value of piston is 20 nm or the RMS value of tip-tilt needs to be less than 0.0155 arcsec when the RMS value of piston is 15 nm if tip-tilt and piston are under non-equal weighting factor. Specific results can be seen in Table 4, Figure 15 and Figure 16.

Table 2 Simulation Results about Piston based on PAOLA

| Theoretical SR of the primary mirror | Theoretical RMS value of piston (nm) | RMS value of Piston in simulation (nm) | SR in simulation |
|--------------------------------------|--------------------------------------|--|------------------|
| 0.92 | 23 | 20 | 0.93 |
| 0.82 | 35.6 | 39 | 0.819 |
| 0.8 | 37.8 | 40 | 0.806 |
| 0.74 | 44 | 45 | 0.736 |
| 0.67 | 53 | 50 | 0.666 |

Table 3 Comprehensive Simulation of Tip-tilt and Piston under Equal Weighting Factor

| RMS value of tip-tilt (arcsec) | RMS value of piston (nm) | SR of primary mirror in simulation |
|--------------------------------|--------------------------|------------------------------------|
| 0.017 | 37.8 | 0.646 |
| 0.014 | 32.3 | 0.72 |
| 0.013 | 28.3 | 0.775 |
| 0.012 | 26.6 | 0.809 |
| 0.009 | 21.1 | 0.88 |

Table 4 Comprehensive Simulation of Tip-tilt and Piston under Non-equal Weighting Factor

| RMS value of piston (nm) | RMS value of tip-tilt (arcsec) | SR of primary mirror in simulation |
|--------------------------|--------------------------------|------------------------------------|
| 20 | 0.014 | 0.807 |
| 20 | 0.015 | 0.806 |
| 20 | 0.016 | 0.796 |
| 15 | 0.0155 | 0.81 |
| 15 | 0.016 | 0.79 |
| 15 | 0.017 | 0.775 |

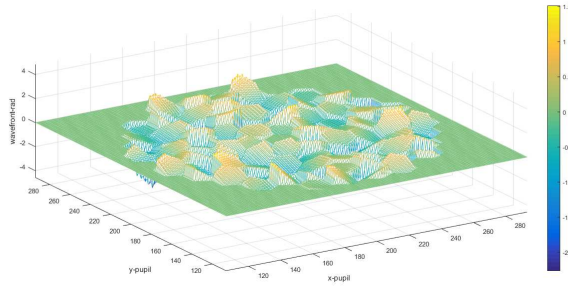


Fig. 13 3D phase diagram of the primary mirror (SR is 0.809 when the RMS value of tip-tilt is 0.012 arcsec and the RMS value of piston is 26.6 nm).

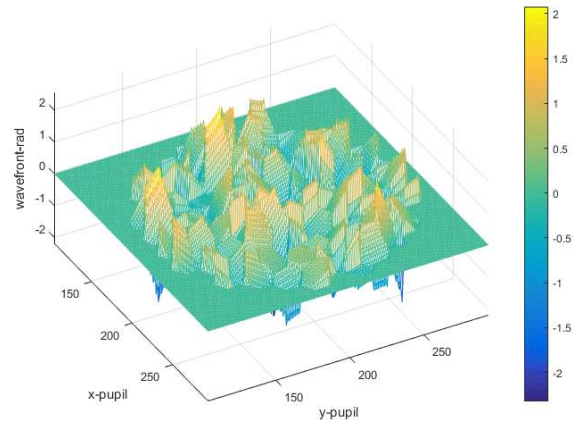


Fig. 15 3D phase diagram of the primary mirror (SR is 0.806 when the RMS value of tip-tilt is 0.015 arcsec and the RMS value of piston is 20 nm).

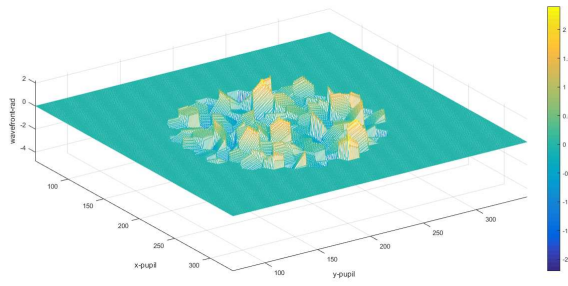


Fig. 14 3D phase diagram of the primary mirror (SR is 0.72 when the RMS value of tip-tilt is 0.014 arcsec and the RMS value of piston is 32.3 nm).

Meanwhile, comprehensive simulation analysis of three out-of-plane errors is done by Zemax. SR of LOT will be larger than 0.8 when the RMS value of tip-tilt is less than 0.013 arcsec and the RMS value of piston is less than 26.5 nm with errors following a normal distribution and having the same weighting factor. Besides, the RMS value of tip-tilt should be less than 0.018 arcsec when the RMS value of piston is 20 nm. The RMS value of tip-tilt

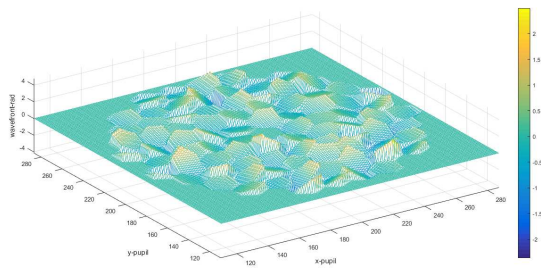


Fig. 16 3D phase diagram of the primary mirror (SR is 0.81 when the RMS value of tip-tilt is 0.0155 arcsec and the RMS value of piston is 15 nm).

Table 5 Comparison of Co-phasing Errors between LOT and Other Segmented Mirror Telescopes

| Telescope | RMS value of tip-tilt (arcsec) | RMS value of piston (nm) |
|----------------------|--------------------------------|--------------------------|
| Keck | 0.018 | 30 |
| TMT | - | 30 |
| ELT | - | 25 |
| LOT (based on PAOLA) | 0.018 | 40 |
| LOT (based on Zemax) | 0.02 | 40 |

should be less than 0.019 arcsec when the RMS value of piston is 15 nm.

In addition, it can be seen from the simulation results from Figure 11 to Figure 16 that high frequency aberrations tend to occur when there are almost no low frequency aberrations. Because this paper only considers the high spatial frequency of segmented mirrors in the active optics of 84 segments, and it does not consider thermal deformation or gravity deformation of segments, there is no analysis of the overall low frequency aberrations (such as overall translation, tilt and defocus).

Co-phasing errors in LOT would be compared with Keck, TMT and ELT, as shown in Table 5. The results demonstrate that the simulation analysis is feasible and correct, which is ready for technical requirements and feasibility of active optics in LOT.

3.3 Comment on the Theory and Methods Used

PAOLA is a program written in IDL language for modeling the performances of an astronomical AO system. PAOLA includes the following functionalities: Segmented pupil with spider structures can be hexagonal, circular or square segments; telescope aberrations can be specified here but only for hexagonal segments. The disadvantages are that PAOLA can only simulate hexagonal, circular or square segments, and PAOLA can only simulate the primary mirror of the entire telescope system. The main advantage of PAOLA over Zemax based on the Monte Carlo method is the extremely short computation time.

The Monte Carlo method is used to analyze the sensitivity of tip-tilt error and piston by Zemax software in order to compare the simulation results from the PAOLA program. Besides, types of segments can be changed by the mask function in Zemax so that we could simulate co-phasing errors of a petal-shaped segmented primary mirror in LOT which is an innovative design solution.

4 CONCLUSIONS

Segmented mirror active optics is the key technical difficulty in the development of LOT when the primary mirror of LOT will achieve diffraction limited resolution in the near-infrared waveband. Out-of-plane co-phasing errors in LOT tiled by hexagonal segments are analyzed theoretically and calculated, and out-plane co-phasing errors are simulated separately and comprehensively with PAOLA and Zemax.

Separate simulation results with Zemax are shown to be more accurate than PAOLA: SR of LOT is larger than 0.8 when the RMS value of tip-tilt obeying a normal distribution is less than 0.02 arcsec, and SR of LOT is larger than 0.8 when the RMS value of piston obeying a normal distribution is less than 40 nm. In addition, comprehensive simulation results with Zemax are summarized as: SR of LOT is larger than 0.8 when the RMS value of piston is less than 26.5 nm and the RMS value of tip-tilt is less than 0.013 arcsec under the condition that tip-tilt obeying a normal distribution and piston obeying a normal distribution have the same weighting factor. SR of LOT is larger than 0.8 when the RMS value of piston is less than 20 nm and the RMS value of tip-tilt is less than 0.018 arcsec. SR of LOT is larger than 0.8 when the RMS value of piston is less than 15 nm and the RMS value of tip-tilt is less than 0.019 arcsec.

The simulation results above are correct and valid. Besides, experiences about segmented mirrors from LAMOST and simulation results in this paper lay a strong theoretical foundation for development of LOT and future large aperture segmented mirror telescopes.

Acknowledgements This work is supported by the National Natural Science Foundation of China (Grant Nos. U1931207, U2031207 and U1931126). The Guoshoujing Telescope (the Large Sky Area Multi-Object Fiber Spectroscopic Telescope, LAMOST) is a National Major Scientific Project built by the Chinese Academy of Sciences. Funding for the project has been provided by the National Development and Reform Commission. LAMOST is operated and managed by the National Astronomical Observatories, Chinese Academy of Sciences.

References

- Baffes, C., Mast, T., Nelson, J., et al. 2008, in *Advanced Optical and Mechanical Technologies in Telescopes and Instrumentation*, SPIE Conference Series, 7018, 70180S
- Chanan, G., Ohara, C., & Troy, M. 2000, *Appl. Opt.*, 39, 4706
- Chanan, G., Troy, M., Dekens, F., et al. 1998, *Appl. Opt.*, 37, 140
- Cui, X.-Q., Su, D.-Q., & Wang, Y.-N. 2003, *IAU Joint Discussion*, 25, E53
- Ellerbroek, B., Britton, M., Dekany, R., et al. 2005, in *Astronomical Adaptive Optics Systems and Applications II*, 5903, 590304
- Geary, J. M. 2002, *Introduction to lens design: with practical ZEMAX examples* (Richmond: Willmann-Bell)
- Gleckler, A. D., & Wizinowich, P. L. 1995, in *Adaptive Optical Systems and Applications*, SPIE Conference Series, 2534, 386
- Jolissaint, L. 2010, *Journal of the European Optical Society*, 5, 10055
- Li, X.-N., Cui, X.-Q., Guo, W.-Y., et al. 2004, in *Optical Fabrication, Metrology, and Material Advancements for Telescopes*, SPIE Conference Series, 5494, 329
- Lightsey, P. A., & Chrisp, M. 2003, in *IR Space Telescopes and Instruments*, SPIE Conference Series, 4850, 453
- Liu, Z., Deng, Y.-Y., Yang, D.-H., et al. 2019, *SCIENTIA SINICA Physica, Mechanica & Astronomica*, 49, 059604 (in Chinese)
- Mast, T. S., & Nelson, J. E. 1982, *Appl. Opt.*, 21, 2631
- McPherson, A., Spyromilio, J., Kissler-Patig, M., et al. 2012, in *Ground-based and Airborne Telescopes IV*, SPIE Conference Series, 8444, 84441F
- Ming, M., Wang, J.-L., Zang, J.-X., et al. 2009, *Optics and Precision Engineering*, 17, 104 (in Chinese)
- Nelson, J. E. 2000, in *Telescope Structures, Enclosures, Controls, Assembly/Integration/Validation, and Commissioning*, SPIE Conference Series, 4004, 282
- Nelson, J. E., & Gillingham, P. R. 1994, in *Advanced Technology Optical Telescopes V*, SPIE Conference Series, 2199, 82
- Piatrou, P., & Chanan, G. 2011, in *Astronomical Adaptive Optics Systems and Applications IV*, SPIE Conference Series, 8149, 814906
- Sanders, G. H. 2013, *Journal of Astrophysics and Astronomy*, 34, 81
- Su, D.-Q., & Cui, X.-Q. 1999, *Progress in Astronomy*, 17, 1 (in Chinese)
- Su, D.-Q., & Cui, X.-Q. 2004, *ChJAA (Chin. J. Astron. Astrophys.)*, 4, 1
- Su, D.-Q., Cui, X.-Q., Wang, Y.-N., & Wang, S.-G. 2000a, in *Telescope Structures, Enclosures, Controls, Assembly/Integration/Validation, and Commissioning*, SPIE Conference Series, 4004, 340
- Su, D.-Q., Liang, M., Yuan, X.-Y., Bai, H., & Cui, X.-Q. 2016, *MNRAS*, 460, 2286
- Su, D.-Q., Liang, M., Yuan, X.-Y., Bai, H., & Cui, X.-Q. 2017, *MNRAS*, 469, 3792
- Su, D.-Q., & Wang, Y.-N. 1997, *Acta Astrophysica Sinica*, 17, 315
- Su, D.-Q., Wang, Y.-N., & Cui, X.-Q. 2004, in *Ground-based Telescopes*, SPIE Conference Series, 5489, 429
- Su, D.-Q., Zou, W.-Y., Zhang, Z.-C., et al. 2000b, in *Optical Design, Materials, Fabrication, and Maintenance*, SPIE Conference Series, 4003, 417
- Troy, M., & Chanan, G. 2003, *Appl. Opt.*, 42, 3745
- Troy, M., Chanan, G. A., Sirko, E., & Leffert, E. 1998, in *Advanced Technology Optical/IR Telescopes VI*, SPIE Conference Series, 3352, 307
- Wan, Y.-J., Yuan, J.-H., Fan, B., & Yang, L. 2007, *Infrared and laser engineering*, 36, 92 (in Chinese)
- Wang, Q.-M. 2015, *PHD Thesis*, Nanjing Institute of Astronomical Optics and Technology University of Chinese Academy of Sciences
- Wang, S.-G., Su, D.-Q., Chu, Y.-Q., Cui, X.-Q., & Wang, Y.-N. 1996, *Appl. Opt.*, 35, 5155
- Yaitskova, N., & Dohlen, K. 2000, in *Optical Design, Materials, Fabrication, and Maintenance*, SPIE Conference Series, 4003, 279
- Yaitskova, N., & Dohlen, K. 2002, *Journal of the Optical Society of America A*, 19, 1274
- Zhang, Y., Wang, Q.-M., Li, Y.-P., et al. 2014a, in *Ground-based and Airborne Telescopes V*, SPIE Conference Series, 9145, 91454Y
- Zhang, Y., Cui, X.-Q., Li, H.-M., et al. 2014b, in *Ground-based and Airborne Telescopes V*, SPIE Conference Series, 9145, 91454W